Available online at www.sciencedirect.com
ScienceDirect
Applied Catalysis B: Environmental 80 (2008) 202–213
APPLIED CATALYSIS B: ENVIRONMENTAL
www.elsevier.com/locate/apcatb

Improvement of catalytic activity and sulfur-resistance of Ag/TiO_2–Al_2O_3 for NO reduction with propene under lean burn conditions

Junhua Li *, Yongqing Zhu, Rui Ke, Jiming Hao

Department of Environmental Science and Engineering, Tsinghua University, Beijing 100084, China

Received 28 October 2006; received in revised form 21 August 2007; accepted 28 August 2007
Available online 4 September 2007

Abstract

Ag-based catalysts supported on various metal oxides, Al_2O_3, TiO_2, and TiO_2–Al_2O_3, were prepared by the sol–gel method. The effect of SO_2 on catalytic activity was investigated for NO reduction with propene under lean burn condition. The results showed the catalytic activities were greatly enhanced on Ag/TiO_2–Al_2O_3 in comparison to Ag/Al_2O_3 and Ag/TiO_2, especially in the low temperature region. Application of different characterization techniques revealed that the activity enhancement was correlated with the properties of the support material. Silver was highly dispersed over the amorphous system of TiO_2–Al_2O_3. NO_3^- rather than NO_2^- or NO*x* reacted with the carboxylate species to form CN or NCO. NO_2 was the predominant desorption species in the temperature programmed desorption (TPD) of NO on Ag/TiO_2–Al_2O_3. More amount of formate ($HCOO^-$) and CN were generated on the Ag/TiO_2–Al_2O_3 catalyst than the Ag/Al_2O_3 catalyst, due to an increased number of Lewis acid sites. Sulfate species, resulted from SO_2 oxidation, played dual roles on catalytic activity. On aged samples, the slow decomposition of accumulated sulfate species on catalyst surface led to poor NO conversion due to the blockage of these species on active sites. On the other hand, catalytic activity was greatly enhanced in the low temperature region because of the enhanced intensity of Lewis acid site caused by the adsorbed sulfate species. The rate of sulfate accumulation on the Ag/TiO_2–Al_2O_3 system was relatively slow. As a consequence, the system showed superior capability for selective adsorption of NO and SO_2 toleration to the Ag/Al_2O_3 catalyst.

Keywords: Selective catalytic reduction of NO; Ag/TiO_2–Al_2O_3; Activity enhancement; SO_2 poisoning; Lewis acid sites

1. Introduction

Nitrogen monoxide (NO) emission from automobile exhaust and industrial waste poses a serious threat to environment since it can cause acid rain and depletion of ozone. A challenging research objective in the field of environmental catalysis is the removal of NO from oxygen-rich exhaust gas from diesel, lean burn gasoline, and natural gas engines. Selective catalytic reduction (SCR) by using of hydrocarbons as a reductant (HC-SCR), a prospective technique to lower NO from lean-burn engines, has been studied widely since the 1990s [1–3].

To date, many kinds of catalysts including noble metal, zeolite and metal oxide were investigated for HC-SCR. Among which, silver on alumina catalysts (Ag/Al_2O_3) seem to be promising [4–8] due to its high activity, selectivity and durability compared to noble metal and zeolite catalysts [9–13]. Ag/Al_2O_3 has showed enhanced NO reduction activity in presence of oxygenated hydrocarbons such as ethanol, acetone, or ether [14–16]. However, there are still two major problems: low-temperature activity and sulfur dioxide poisoning. It is difficult to ensure sufficient catalyst activity to remove NO at the low temperature range of the diesel engine exhaust. SO_2 in the exhaust gas can poison catalysts and drastically lower their effectiveness. In order to increase the operation temperature range and improve low-temperature NO conversion, some work has been devoted to adding a second element to active sites. For example, the addition of 0.01 wt.% Pd into a 5 wt.% Ag-based SCR catalyst increased the reaction activity of NO at low temperatures, both in the absence and presence of SO_2 [17]. Son et al. [18] studied the effect of adding alkali metals (Li, Na, K, Cs) to Ag/Al_2O_3, and found that the activity was slightly improved by the addition of either 0.5 wt.% Cs or 1 wt.% Cs to

* Corresponding author. Tel.: +86 10 627 82030; fax: +86 10 62785687.
E-mail address: lijunhua@tsinghua.edu.cn (J. Li).

0926-3373/$ – see front matter © 2007 Elsevier B.V. All rights reserved.
doi:10.1016/j.apcatb.2007.08.016

2 wt.% Ag/Al_2O_3. However, the enhancement of activity was insufficient for practical applications.

The tolerance of Ag-based catalysts to SO_2 depends on the type and oxidation state of silver, as well as the nature of the chemical addition. Most researchers reported that the presence of SO_2 in the feed gas significantly and permanently lowered the NO reduction activity. Meunier et al. [10] studied the effects of SO_2 on Ag/Al_2O_3 activity for NO reduction with propene. The nitrogen yield and propene conversion over the catalyst decreased significantly after exposure to 100 ppm SO_2. Sumiya et al. [19] examined the effect of H_2O and SO_2 on the activity of Ag/Al_2O_3 mounted on a cordierite. The suppression of the NO reduction activity in the presence of SO_2 is attributed to the formation of sulfates on the catalyst. The decrease in activity is caused by the sulfation of the silver species that is responsible for the formation of a key intermediate (ad-NO*x*) in the reaction mechanism. Gandhi and Shelef [20] investigated the effect of sulfur and sulfur compounds on the reduction of NO. They also concluded that under oxidizing conditions, the sulfur storage capability in the form of sulfate directly affected sulfur-resistance of the catalyst.

Meunier et al. [9] proposed a different mechanism that is dependent on types of Ag phase. Large Ag^0 particles formed at high silver loading can catalyze the decomposition of NO whereas Ag^+ species prevailing on low loading favors the oxidation of NO to ad-NO_x species, which subsequently reacts through the intermediate organo-nitrogen compounds. It is also found that the reduction of the ad-NO_x species or NO_2 by propene occurs mostly on the alumina surface in either the oxide or aged form [10,12]. However, there is no conclusive consensus regarding the influence of SO_2 on Ag-based catalysts due to the different experimental conditions and conflicting results reported in the literature. For instance, some researchers found a promotional effect on the catalyst activity in the presence of SO_2. Angelidis et al. [21] also observed a promotional effect on the catalytic reduction of NO over 5 wt.% Ag/Al_2O_3 under the operation conditions of 100 ppm SO_2, excessive oxygen and a mixture of propane/propene. The authors ascribed the promotional effect to the formation of hydrocarbon oxygenates caused by SO_2. Park and Boyer [13] studied the effect of SO_2 on the activity of Ag/Al_2O_3 with various Ag loadings on a C_3H_6-SCR for NO. The authors concluded that the improvement of the NO conversion might be due to the formation of Ag_2SO_4 phase from silver oxide. They claimed that Ag_2SO_4 could produce more –NCO species and suppress propene oxidation than Ag_2O. The decrease of catalytic performance in presence of SO_2 was mainly due to the poisoning of alumina active sites which are responsible for NO reduction to N_2. It is concluded that the addition of SO_2 enhanced the performance of silver sites, but hindered the NO reduction function of alumina sites. Therefore, a future study should focus on development of a sulfur resistant alumina material in an attempt to improve catalyst resistance against SO_2 poisoning.

TiO_2, as a support for the commercial catalyst (V_2O_5/TiO_2) has been widely used for the selective catalytic reduction of NO with ammonia for stationary sources. The catalyst exhibits high catalytic activity and tolerance to SO_2. Al_2O_3, containing mixed support oxides like $TiO_2 + Al_2O_3$ for hydrodesulfurization catalysts have been studied to improve the sulfur-resistance [22–24]. Because of the advantage of sulfur-resistant TiO_2 and the high specific area of Al_2O_3, it is worthwhile to investigate the Ag-based catalytic material on a TiO_2–Al_2O_3 composite support for lean NO reduction, and to clarify the mechanisms of various supports and SO_2 impacts on catalyst performance.

In this paper, silver on TiO_2, Al_2O_3, and TiO_2–Al_2O_3 supports (1:1 in mass weight) were prepared by the sol–gel method, and characterized by X-ray diffraction (XRD), X-ray photoelectron spectroscopy (XPS), Transform electronic micrograph (TEM), Temperature programmed desorption (TPD), and in situ Fourier transformed infrared (FT-IR) spectroscopy. It was found that the active component of silver was well dispersed in the amorphous system of TiO_2–Al_2O_3, and the activity was obviously enhanced on the TiO_2–Al_2O_3 composite, especially in the low temperature region. The information derived from these characterization techniques has been correlated the catalyst performance in order to understand the activity enhancement of Ag/TiO_2–Al_2O_3 and SO_2 on catalyst performance.

2. Experimental

2.1. Catalyst preparation

Several silver-based catalysts, namely Ag/Al_2O_3, Ag/TiO_2 and Ag/TiO_2–Al_2O_3, were prepared by single step sol–gel procedure reported previously [25]. Briefly, aluminium boehmite sol was prepared by hydrolysis of aluminium (III) iso-propoxide (AIP) in hot water (358 K) with a small amount of nitric acid until it formed the sol. Subsequently, the required amount of tetrabutyl titanate sol was added to the aluminium boehmite sol with vigorous stirring for half an hour. A silver nitrate solution was incorporated into the sol by stirring for 6 h. The solvents were removed by heating under reduced pressure to form a gel. This gel was dried at 358 K for 24 h, followed by calcination at 823 K for 3 h in air. The ratio of TiO_2 to Al_2O_3 in mass fraction was 1:1 for Ag/TiO_2–Al_2O_3 catalysts, and Ag loadings was 5 wt.% for all samples.

2.2. Catalytic performance test

The activity measurements were carried out in a fixed-bed quartz reactor (inner diameter 8 mm) using a 0.25 g catalyst of 60–80 mesh. The feed gas mixture contained 800 ppm NO, 800 ppm C_3H_6, 8% O_2, 0 or 2% H_2O, 0 or 100 ppm SO_2, and N_2 as the balance gas. H_2O was introduced through a saturator, cooled and removed after the reactor. The total flow rate of the feed gas was 100 $cm^3\ min^{-1}$, corresponding to a space velocity of about 18,000 h^{-1}. The fresh catalyst was pretreated at 773 K for 12 h in the reaction gases with 100 ppm SO_2, to achieve an aged catalyst. NO and NO_2 concentration were analyzed with a Chemiluminescence NO/NO_2 Analyzer (Thermal Environmental Instruments, model 42C). Other product gases were analyzed using a Mass Spectrograph (Omnistar) or Shimadzu

GC 17A equipped with Porapak Q and Molecular sieve 5A columns. N_2O concentration was too low (<10 ppm) to be detected by GC equipped with Porapak Q in this work.

2.3. Catalyst characterization

BET-surface areas were measured by N_2 adsorption using a NOVA4000 automated gas sorption system. XRD measurements were carried out on a Rigaku D/MAX-RB X-ray Diffractometer with Cu Kα radiation. XPS measurements were conducted on a PHI15300/ESCA system with Al Kα radiation (1484.6 eV), calibrated internally by carbon deposit C 1s binding energy (BE) at 284.6 eV. The atomic quantification results were calculated with the software on PHI15300/ESCA system. TEM measurements were performed in a JEOL JEM-2010 apparatus, with the accessory of LINK ISIS-300 EDS.

2.4. TPD

Temperature programmed desorption experiments of NO were carried out by using a 100 mg catalyst sample. Prior to the NO TPD experiment, the catalyst sample was pretreated in a flow of 8% O_2/N_2 at 873 K for 1 h and then was cooled down to room temperature. Chemisorption of NO was performed by passing a flow of 800 ppm NO and 8% O_2 diluted in N_2 through the sample bed at room temperature for 1 h. After the sample was purged with N_2 until no NO was detected by a Chemiluminescence NO/NO_2 Analyzer (Thermal Environmental Instruments, model 42C), the TPD measurements were carried out up to 873 K with a heating rate of 10 K min^{-1} in flowing N_2. The gas flow rate was fixed at 100 cm^3 min^{-1}. The amount of NO desorbed from the catalyst was quantified with a specific software by calibrating the peak area.

TPD of SO_2 was performed by using a 100 mg catalyst sample and SO_2 was tested by flue gas analyzer (Quint OX). The pre-treatment was with the same procedure as mentioned above. Chemisorption of SO_2 was performed by passing a flow of 100 ppm SO_2 and 8% O_2 diluted in N_2 through the sample bed at room temperature for 2 h. After the sample was purged with N_2 until no SO_2 was detected, the TPD measurements were carried out up to 1073 K with a heating rate of 10 K min^{-1} in flowing N_2. The gas flow rate was controlled at 200 cm^3 min^{-1}.

2.5. FT-IR and DRIFTS analysis

The FT-IR spectra of chemisorbed pyridine (Py-IR) were obtained in-situ reactor cell of a Perkin-Elmer Model 2000 spectrophotometer in the 1800–1100 cm^{-1} range. The self supported sample wafers were out-gassed at 773 K for 1 h prior to pyridine adsorption. After the adsorption of pyridine at room temperature, the samples were out-gassed at 373, 423, 473, 573 and 673 K and their spectra were recorded.

In situ DRIFTS spectra were recorded on a NEXUS 670-FTIR. The samples were finely ground and placed in a ceramic crucible. The feed gas streamed into the cell at a total flow rate of 100 cm^3 min^{-1}. The samples were preheated in N_2 and O_2 for 60 min. The background spectra were collected after subjected to the desired temperature for 30 min. The sample spectra reported here were collected after being exposed for 30 min. In all cases, 100 scans were recorded at a resolution of 4 cm^{-1}.

3. Results

3.1. Effect of the support on catalyst performance

Fig. 1 shows the results of selective catalytic reduction of NO with propene over Ag-based catalysts with various kinds of supports in the absence of SO_2. It can be seen that the catalytic activities of Ag/TiO_2 are low over the entire temperature range, and the maximum NO conversion is only about 10% near 673 K. In comparison, on Ag/Al_2O_3 and Ag/TiO_2–Al_2O_3 catalysts, NO conversions are much higher than that on Ag/TiO_2, and the maximum NO conversions reach above 90% on both Ag/Al_2O_3 and Ag/TiO_2–Al_2O_3. More significantly, the better operating window was obtained over silver on binary metal oxide TiO_2–Al_2O_3, and the catalytic activities at lower

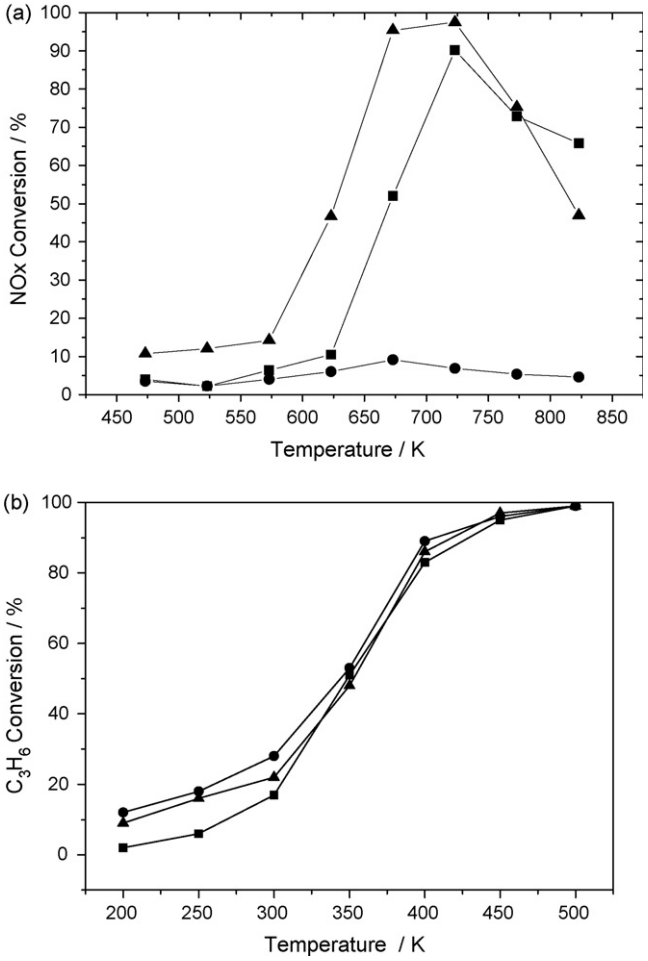

Fig. 1. The effect of various supports on catalytic activities for SCR of NO with propene in the absence of SO_2. (a) NO conversion, (b) C_3H_6 conversion. Reaction conditions: 800 ppm NO, 800 ppm C_3H_6, 8% O_2, 2% H_2O, N_2 as balance gas, W/F = 18,000 h^{-1}. (■) 5 wt.% Ag/Al_2O_3; (●) 5 wt.% Ag/TiO_2; (▲) 5 wt.% Ag/TiO_2–Al_2O_3.

temperatures (<673 K) were enhanced remarkably compared to single metal oxide catalysts. For example, the NO conversions over $Ag/TiO_2–Al_2O_3$ increased by 40% at 625 and 673 K compared to Ag/Al_2O_3, and NO conversion over $Ag/TiO_2–Al_2O_3$ reached nearly 100% at 723 K. The results of C_3H_6 conversions showed that the propene was completely consumed at 773 K over all catalysts. However, propene is more easily oxidized on the catalyst with TiO_2 or $TiO_2–Al_2O_3$ supports than Al_2O_3.

3.2. Effect of SO_2 on catalytic activity

Because of high activity for NO reduction, Ag/Al_2O_3 and $Ag/TiO_2–Al_2O_3$ catalysts were further studied to determine the effect of SO_2 on selective catalytic reduction of NO with propene. Fig. 2 shows the catalytic activities over fresh and aged samples in the presence of SO_2 over the temperature range of 473–823 K. It can be seen that the $Ag/TiO_2–Al_2O_3$ catalyst exhibits better activity at lower temperature. A wider window of activity than that on Ag/Al_2O_3 is also reached in the presence of SO_2.

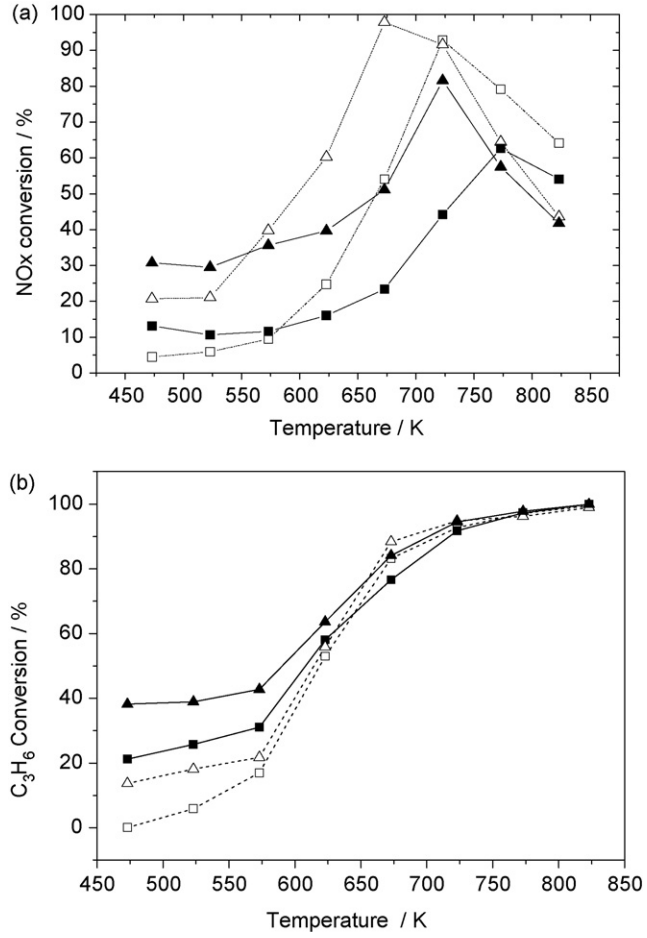

Fig. 2. SO_2 effects on catalytic activities for SCR of NO with propene over various catalysts. (a) NO conversion, (b) C_3H_6 conversion. Reaction conditions: 800 ppm NO, 800 ppm C_3H_6, 8% O_2, 100 ppmSO_2, N_2 as balance, W/F = 18,000 h^{-1}. (□△) with 100 ppm SO_2 on fresh catalyst; (■▲) with 100 ppm SO_2 on sulfated catalyst (100 ppm SO_2 poisoned at 723 K for 12 h); (■□) Ag/Al_2O_3; (▲△) $Ag/TiO_2–Al_2O_3$.

On fresh samples, no obvious decrease of the maximum value of NO conversion was observed on both Ag/Al_2O_3 and $Ag/TiO_2–Al_2O_3$ by adding 100 ppm SO_2 to the feed gas (see Figs. 1 and 2). In contrast, the maximum value of NO conversions decreased on both Ag/Al_2O_3 and $Ag/TiO_2–Al_2O_3$ in the presence of 100 ppm SO_2. However, the decrease of catalyst activity on $Ag/TiO_2–Al_2O_3$ (18%) is much lower than on Ag/Al_2O_3 (about 30%). The peak temperature shifted by 50 K to the high temperature region, which is from 723 to 773 K on Ag/Al_2O_3 and 673 to 723 K on $Ag/TiO_2–Al_2O_3$. It was interesting that the activity at low temperatures (<523 K) was greatly enhanced on the aged samples. Compared with the fresh catalyst evaluated in the absence of 100 ppm SO_2, the activity at low temperatures was improved slightly on the fresh catalyst at the SO_2 concentration of 100 ppm, but the activity improvements was obvious on the aged samples. For $Ag/TiO_2–Al_2O_3$, the conversion NO to N_2 for the aged sample increased more than 20% at 473 K compared to the fresh catalyst (see Figs. 1 and 2). In comparison, on the Ag/Al_2O_3 catalyst, in spite of activity increase at low temperature, the improvement is lower than for $Ag/TiO_2–Al_2O_3$, which shows 30% more NO conversion than Ag/Al_2O_3 below 673 K.

In Fig. 2b, for both Ag/Al_2O_3 and $Ag/TiO_2–Al_2O_3$, C_3H_6 conversions greatly increased on aged samples compared to fresh catalysts in the low temperature region. In comparison, C_3H_6 conversion on $Ag/TiO_2–Al_2O_3$ was much higher than that on Ag/Al_2O_3 in the low temperature region. The conversion of NO to N_2 almost reached 40% at 473 K on aged $Ag/TiO_2–Al_2O_3$ while it was only 22% on the aged Ag/Al_2O_3 sample. At the reaction temperature above 623 K, C_3H_6 conversions on fresh catalyst were higher than those of aged catalyst. Finally, C_3H_6 was almost completely consumed at 773 K. This indicates that the activity improvement might be ascribed to the activation of propene. $TiO_2–Al_2O_3$ shows a higher capability to propene oxidation and better tolerance to SO_2 than Al_2O_3. The activities were significantly promoted for NO reduction with propene, especially on the aged sample at low temperatures in the presence of SO_2 compared with Ag/Al_2O_3.

3.3. Catalyst characterization

3.3.1. BET surfaces

The physical properties of various catalysts are summarized in Table 1. The surface area of Ag/Al_2O_3 is 223 $m^2\ g^{-1}$, and silver on the binary metal oxide $TiO_2–Al_2O_3$ catalyst did not cause a decrease of surface area. Instead, the surface area showed a slight increase (from 223 to 226 $m^2\ g^{-1}$), although the

Table 1
Surface area and pore volume test

Samples	Ag/Al_2O_3		$Ag/TiO_2–Al_2O_3$		Ag/TiO_2
	Fresh	Aged	Fresh	Aged	
Specific area (m^2 g)	223	186	226	203	64
Average pore diameter (nm)	4.1	3.9	6.4	6.1	3.7
Pore volume ($cm^3\ g^{-1}$)	0.21	0.20	0.48	0.46	0.20

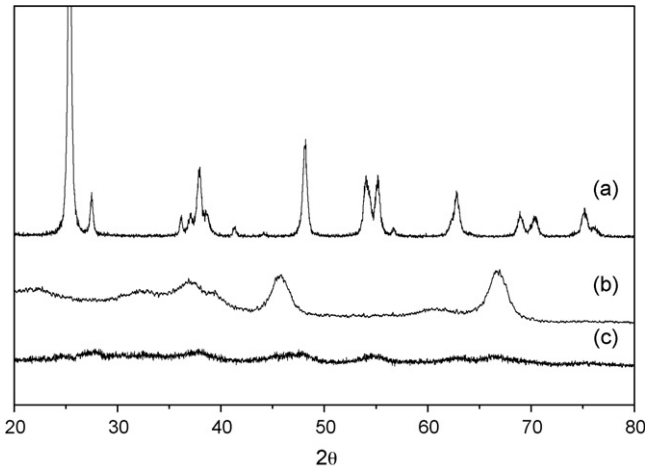

Fig. 3. X-ray diffraction patterns of Ag-based catalysts with various supports. (a) Ag/TiO_2, (b) Ag/Al_2O_3, (c) Ag/TiO_2–Al_2O_3.

surface area of Ag/TiO_2 was only about 64 $m^2\ g^{-1}$. Ag/TiO_2–Al_2O_3 showed the highest pore volume of 0.48 $cm^3\ g^{-1}$ and average pore diameter 6.4 nm among the three catalysts. In comparison, silver, on the single metal oxide supports of Al_2O_3 and TiO_2, caused a significant decrease for pore volume. These single metal oxides have less than half the pore volume of the binary metal oxide support. The aged catalyst indicates a slight decrease of the surface area and pore volume both on Ag/Al_2O_3 and Ag/TiO_2–Al_2O_3; these can be ascribed to a blockage of the pores by the accumulated sulfur.

3.3.2. XRD

The X-ray diffraction patterns of the various catalysts taken in the range of 10–90° are shown in Fig. 3. The peaks of Ag/TiO_2 showed a typical anatase phase TiO_2 with little rutile phase according to the related literature, and the peaks of Ag/Al_2O_3 were mainly assigned to the γ-Al_2O_3 phase [22,24]. Notably, the XRD pattern of Ag/TiO_2–Al_2O_3 shows a nearly an amorphous system. This phenomenon was also observed at a binary metal oxide of In_2O_3–SnO_2 catalyst (1:1 in mass ratio) for complete oxidation of methane [26]. The above observations indicate that the silver species were well dispersed on the supports since neither Ag nor Ag^+ was detected. In addition, TiO_2 was well incorporated into Al_2O_3 and then the particle size may be smaller, the amorphous phase and the small size of the support also contributed to the significant dispersion of active sites.

3.3.3. XPS

Table 2 summarized the XPS experimental and theoretical results of the atom concentration of the surface for the Ag/TiO_2–Al_2O_3 catalyst. The experimental results of atom concentration for O1s and Ag3d were significantly higher than indicated by the theoretical results. This behavior could be due to the enrichment of Ag and O on the surface. On the contrary, the atom concentration for Ti2p and Al2p were much less than that suggested by theoretical results. Considering the atomic surface ratio for Ti/Al catalyst, the XPS experimental results were 0.47 while the theoretical result was 0.62. With respect to the binding energies (BE) of the aluminum and titanium elements also given in Table 2, they were reported in the literature as 74.3 and 458.7 eV, respectively. The literature values are in good agreement with those obtained in this work for the Ag/TiO_2–Al_2O_3 sample, therefore, the compound formation of Ti and Al are still TiO_2 and Al_2O_3, and no new composite solid solution was formed. This result is also confirmed by the XRD spectra.

Table 2
XPS results for Ag/TiO_2–Al_2O_3 catalyst

	Ti2p	Al2p	Ag3d	O1s
Atomic concentration	8.90	18.75	0.94	71.42
Theoretical	14.18	22.98	0.55	62.30
Binding energies (eV)				
Ag/TiO_2–Al_2O_3	458.7	74.3	368.0	530.8
TiO_2[a]	458.7			529.9
Al_2O_3[a]		74.3		531.3
Ag_2O[a]			367.8	529.2

[a] From Handbook of X-Ray Photoelectron Spectroscopy, C.D. Wagner, W.M. Riggs, L.E. Davis, J.F. Moudler, G.E. Muilenberg (Eds.), Perkin-Elmer, 1978, pp. 50, 68.

3.3.4. TEM and EDS

Fig. 4a and b display the transmission electron microscopy corresponding to the Ag/Al_2O_3 and Ag/TiO_2–Al_2O_3 catalysts, respectively. The technique involving light fields was used allowing identification of metal particles (dark points). From Fig. 4a, the conglomeration of Ag could be seen (circled in figure) and the average diameter of silver was about 10 nm. This conglomeration of Ag, however, was not observed in Ag/TiO_2–Al_2O_3 catalyst in Fig. 4b. The results might indicate that Ag was well dispersed on the binary metal oxide support compared to the alumina support; the possible reason is that the binary metal oxide is amorphous and titanium oxide was well incorporated and dispersed on alumina.

Fig. 5 shows a typical electron diffraction pattern of Ag/TiO_2–Al_2O_3, and the diffraction rings are obviously evident. It is suggested that the size of metal oxide was very small, and it was an amorphous system which was confirmed in the XRD results (Fig. 3). This indicated that TiO_2 was well incorporated into Al_2O_3 just as the Al_2O_3 was thoroughly mixed with the TiO_2, and then the silver species were well dispersed in the amorphous system of TiO_2–Al_2O_3.

Table 3 summarizes the results of EDS elemental analysis of the Ag/Al_2O_3 and Ag/TiO_2–Al_2O_3 catalysts. On the aged Ag/Al_2O_3 sample, the concentration of sulfur was 1.82%, while on the aged Ag/TiO_2–Al_2O_3 sample sulfur concentration was only 0.84%. The binary metal oxide (addition of TiO_2) suppressed the formation of surface sulfate species, which is in accordance with the results of SO_2-TPD.

3.4. TPD profiles

3.4.1. TPD of NO

Fig. 6 illustrates TPD profiles of NO and NO_2 obtained on Ag/Al_2O_3 and Ag/TiO_2–Al_2O_3 catalysts for various conditions,

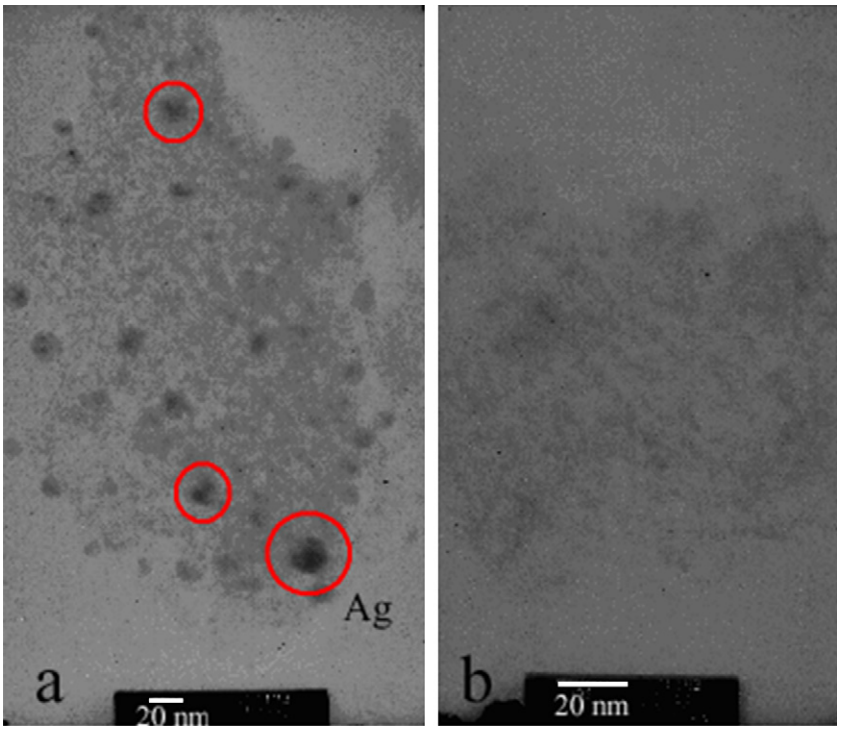

Fig. 4. TEM micrographs of Ag/Al_2O_3 (a) and Ag/TiO_2–Al_2O_3 (b).

namely, TPD of NO on fresh catalyst (a), TPD of NO on aged sample (b), and TPD of NO adsorption with SO_2 on aged sample (c). The amount of NO_x desorption over various catalysts is summarized in Table 4. For Ag/Al_2O_3, two peaks were observed. The first peak was centered at about 373 K and the second one was around 723 K. The former peak might be due to the decomposition of weak adsorption species (nitrite and NO) because NO was the predominant specie of NO_x, while the later peak might be due to strong adsorption species (nitrate species) decomposition because most of the NO_x desorption specie was NO_2, and the desorption of NO_2 at high temperature was accompanied with the desorption of O_2 [27,28]. On the aged sample, the weak adsorption of NO_x at low temperature increased; however, the strong adsorption species decreased. Regarding NO co-adsorption with SO_2 on the aged sample, the first peak increased significantly while the second peak substantially decreased. The amount of total NO_x adsorption was 372, 343 and 336 μ mol g^{-1} corresponding to those of a fresh catalyst (a), aged sample (b), and NO adsorption with SO_2 on aged sample (c). For the strong adsorption species, the results were 301, 235 and 126 μ mol g^{-1} from curves (a)–(c) integrally calculated in the region of 473–873 K.

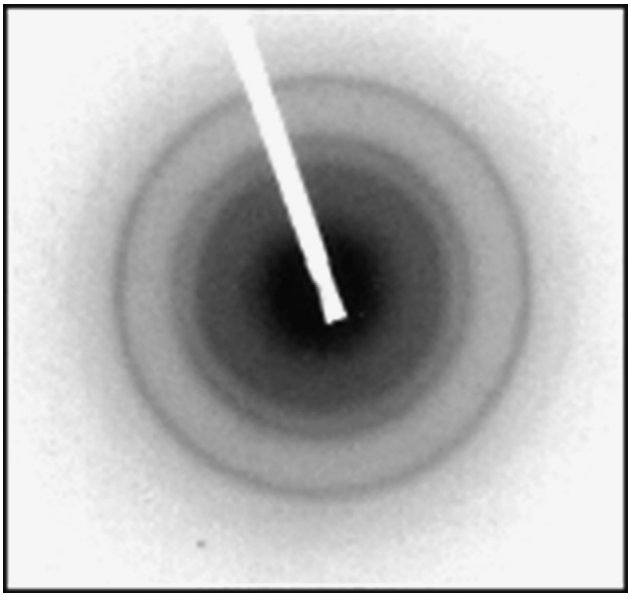

Fig. 5. The selected area electron diffraction patterns of Ag/TiO_2–Al_2O_3.

In comparison, it is interesting that the NO adsorption on Ag/TiO_2–Al_2O_3 was mainly concentrated in the high temperature region. The adsorption of the weak adsorption species was very little compared to adsorption on Ag/Al_2O_3. This indicates that the surface adsorption species might be mainly nitrate. The adsorption species on the aged sample was slightly less than on the fresh sample, and the peak temperature shifted to a low temperature region. For NO co-adsorption with SO_2 on the aged Ag/TiO_2–Al_2O_3 sample, the amount of NO adsorption decreased. However, the amount of adsorption of NO_x was still

Table 3
EDS elemental analysis of the Ag/Al_2O_3 and Ag/TiO_2–Al_2O_3 catalysts

Elements (wt.%)	Ag/Al_2O_3		Ag/TiO_2–Al_2O_3	
	Fresh	Aged	Fresh	Aged
O	53.1	54.5	35.2	35.6
Al	36.6	37.8	32.7	32.9
Ag	6.24	5.91	4.96	6.39
Ti	–	–	27.0	24.2
S	–	1.82	–	0.840

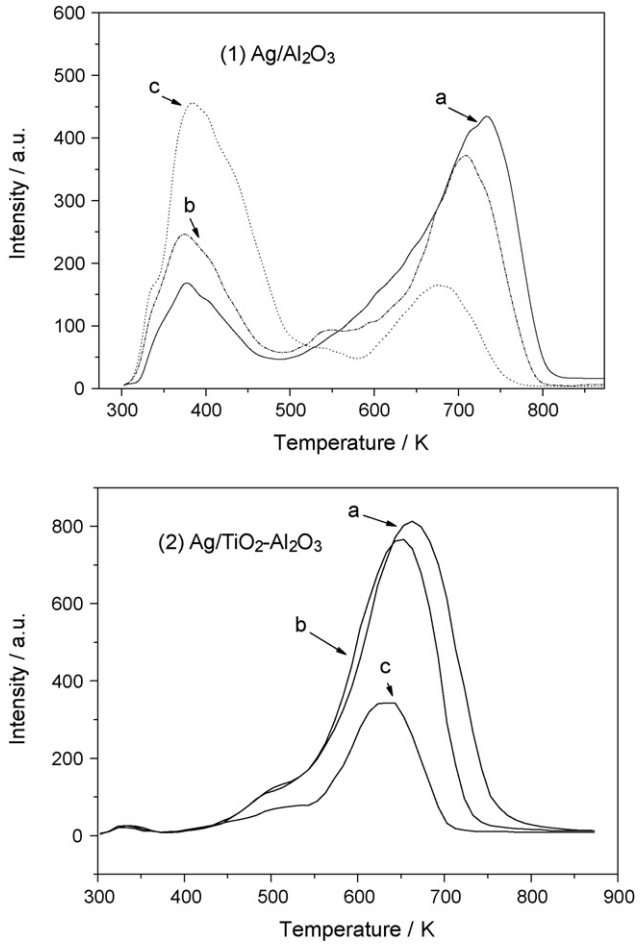

Fig. 6. TPD profiles of NO on Ag/Al_2O_3 (1) and Ag/TiO_2–Al_2O_3 (2) catalysts. (a) TPD of NO on fresh catalyst, (b) TPD of NO on aged sample, (c) TPD of NO adsorption with SO_2 on aged sample.

higher than that on Ag/Al_2O_3 over the high temperature region. Over the entire temperature range of 473–873 K, the amount of total NO_x adsorption were 525, 444, 182 μ mol g^{-1} for a fresh catalyst (a), TPD of NO on aged sample (b), TPD of NO adsorption with SO_2 on aged sample (c), respectively.

Various kinds of support showed different TPD profiles. The results in Table 4 show that the amount of adsorption of NO_x on Ag/TiO_2 is very little mainly due to the small specific area. On the aged Ag/Al_2O_3 sample, the adsorption of nitrate species was slightly less than that of the fresh sample, while the amount of adsorption of the nitrate species greatly decreased in co-existence with SO_2. However, the amount of adsorption of the nitrate species was larger on Ag/TiO_2–Al_2O_3 in the 473–873 K region than that of Ag/Al_2O_3.

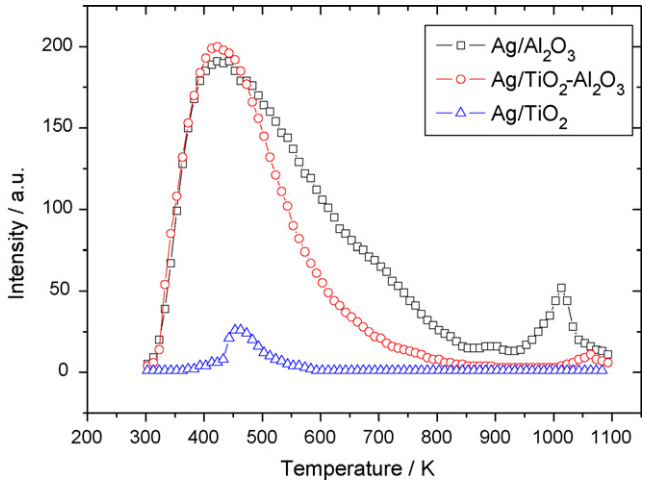

Fig. 7. TPD profiles of SO_2 on Ag-based catalyst supported on Al_2O_3, TiO_2 and TiO_2–Al_2O_3.

3.4.2. TPD of SO_2

Fig. 7 illustrates the TPD profiles of SO_2 obtained on Ag/Al_2O_3, Ag/TiO_2 and Ag/TiO_2–Al_2O_3 catalysts. The decrease order of the peak intensity of SO_2-TPD is Ag/Al_2O_3, Ag/TiO_2–Al_2O_3 and Ag/TiO_2, and the total amounts of SO_2 adsorption were 537, 392, and 28.7 μ mol g^{-1}, respectively. The main adsorption peaks were around 450 K, which might be the weak adsorption of SO_2 on the alkali sites. However, on Ag/Al_2O_3 catalyst, there was another absorption peak around 1010 K. The second peak might be due to the decomposing of sulfate on the surface of catalyst [29]. In contrast, it is obvious that the second absorption peak was very small on Ag/TiO_2–Al_2O_3 catalyst, and it almost disappeared on Ag/TiO_2. This indicates that the sulfate might be surface $Al_2(SO_4)_3$ because it is hardly decomposed in the reaction temperature region. Therefore, the effect of the type of support on the adsorption of SO_2 is significant as the SO_2 adsorption occurred selectively on various support. Because the adsorption of NO_x is large on Ag/TiO_2–Al_2O_3 and the adsorption of SO_2 is lower than that on Ag/Al_2O_3, the selective adsorption of NO and SO_2 is associated with the support. TiO_2–Al_2O_3 support suppressed the formation of sulfate species on the catalyst surface due to the TiO_2 addition into the Al_2O_3. This result is in agreement with the results of elemental S concentration detected by EDS.

Table 4
The amount of NO_x adsorption over various catalysts (μ mol g^{-1})

Adsorption		Ag/Al_2O_3	Ag/TiO_2–Al_2O_3	Ag/TiO_2
On fresh sample in the absence of SO_2	The amount of NO_x	372	541	70.5
	473–873 K	301	525	53.9
On aged sample in the absence of SO_2	The amount of NO_x	343	461	16.3
	473–873 K	235	444	10.8
On aged sample in the presence of SO_2	The amount of NO_x	336	197	6.32
	473–873 K	126	182	3.81

3.5. FT-IR

3.5.1. Py-IR

Pyridine has been used as a probe for the determination of the nature of the acid sites on the surface of catalysts. The results on fresh and aged catalysts are shown in Figs. 8 and 9, respectively. The stretching bands of infrared spectrum of pyridine adsorbed on solid acids have been clearly identified. The bands at 1451, 1493, and between 1600 and 1630 cm^{-1} correspond to different modes of vibration of pyridine coordinated to the Lewis acid sites. The band at 1545 cm^{-1} has been assigned to the pyridine in Brønsted acid sites (not detected in this figure). The band at 1490 cm^{-1} is characteristic of the Lewis–Brønsted acid complex. On these samples, only Lewis acid sites were identified although the Brønsted acid site was observed in the former report [30]. With increasing temperature, the peaks steadily decreased, and almost disappeared at 673 K.

The intensity of the Lewis acid sites was enhanced significantly on aged Ag/Al_2O_3 and Ag/TiO_2–Al_2O_3 samples compared to the fresh samples. For different sulfate component, the wave number of the S=O band changed from 1352 to

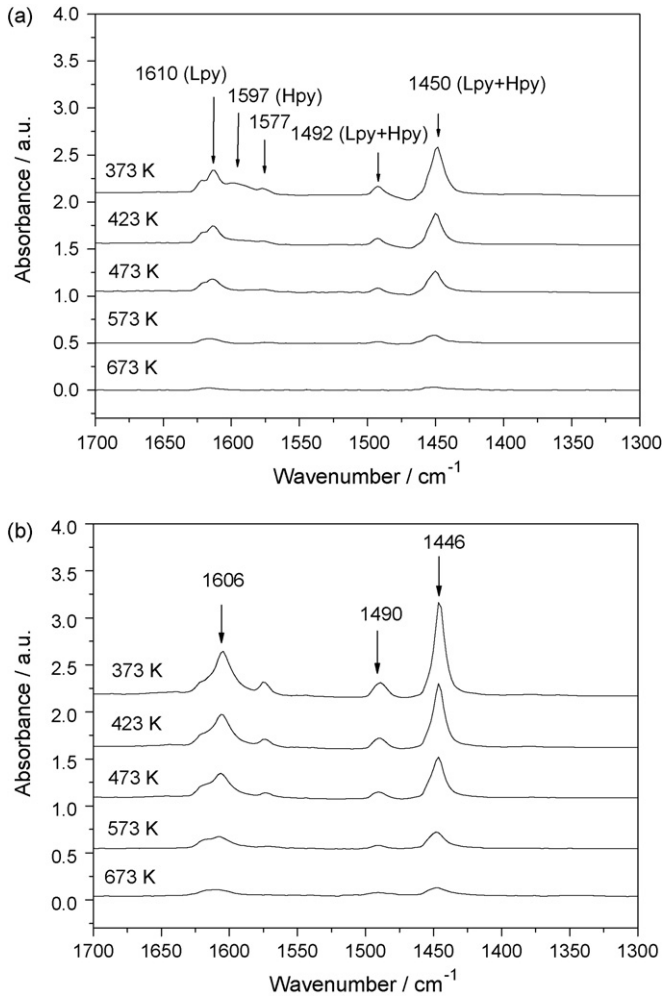

Fig. 8. Infrared spectra of pyridine adsorbed on fresh catalysts. (a) Ag/Al_2O_3; (b) Ag/TiO_2–Al_2O_3.

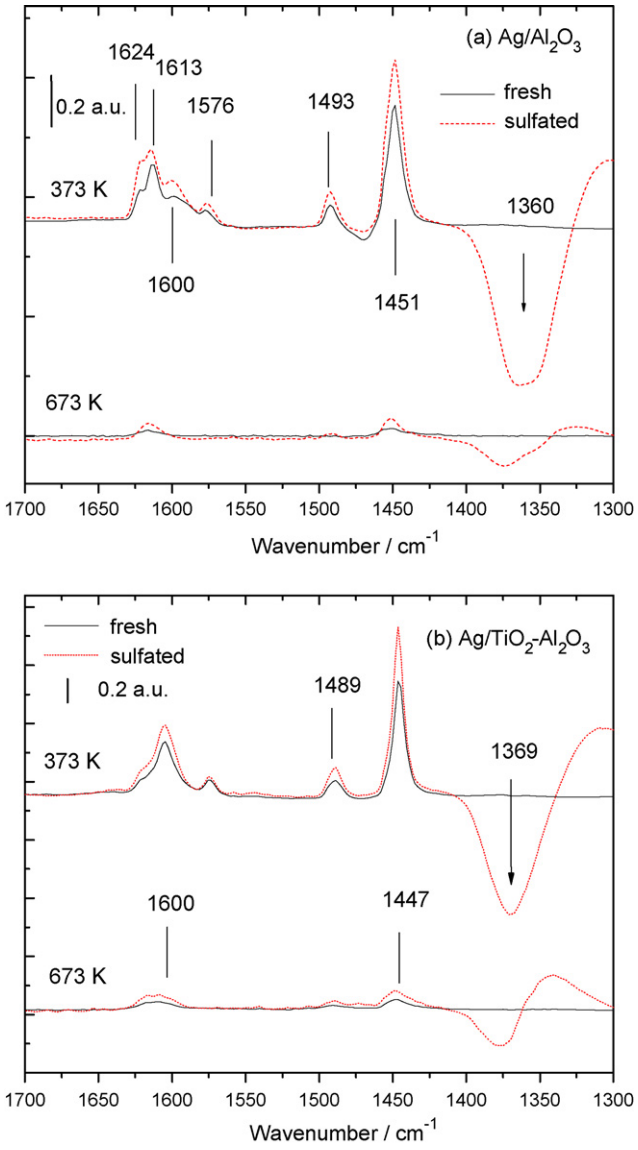

Fig. 9. Comparison of Infrared spectra of pyridine adsorbed on fresh and aged Ag/Al_2O_3 (a) and Ag/Al_2O_3–TiO_2 (b) at 373 and 673 K.

1402 cm^{-1}. The bands at low wave numbers are assigned to isolated surface (SO_4^{2-}) groups whereas the band around 1400 cm^{-1} is tentatively attributed to the $S_2O_7^{2-}$ species [31,32]. The S=O band was also weakened when the temperature increased from 373 to 673 K.

For both fresh and aged samples, the intensity of Lewis acid sites of Ag/TiO_2–Al_2O_3 was much higher than that of Ag/Al_2O_3. This indicates that the strength of Lewis acid sites was substantially related to the support material, and the catalyst performance was related to the Lewis acid sites.

3.5.2. DRIFTS results

Fig. 10 shows the in situ DRIFTS spectra of fresh Ag/Al_2O_3 and Ag/TiO_2–Al_2O_3 catalysts in the flow of NO + C_3H_6 + O_2 at a steady-state for various temperatures. The in situ DRIFTS spectra on Ag/TiO_2 samples was also carried out (not shown here), however, the absorption of surface species was too weak to be recognized.

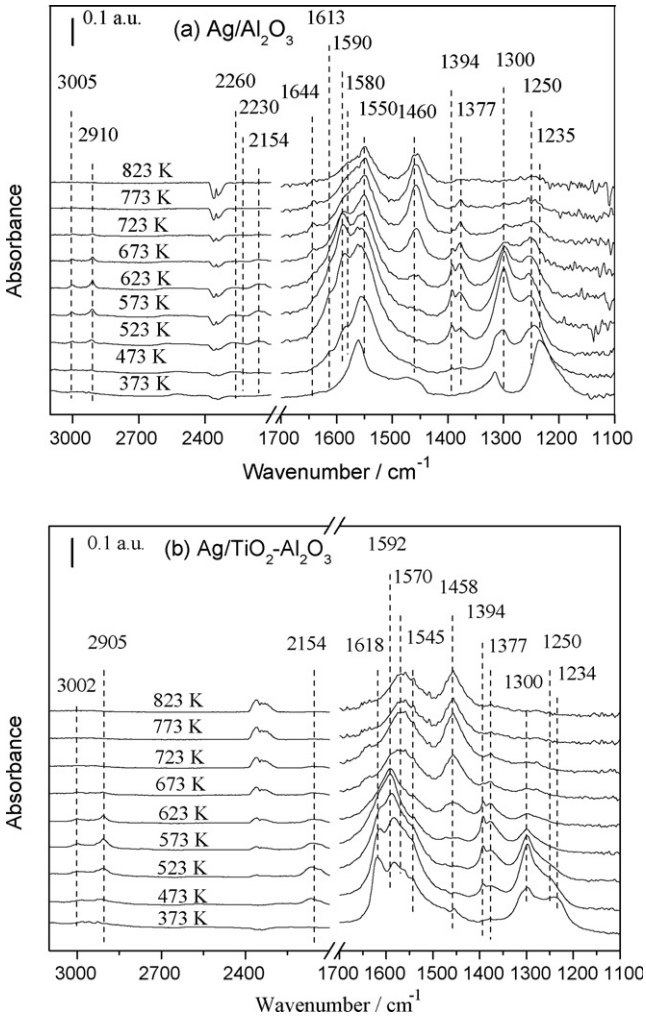

Fig. 10. In-situ steady-state DRIFTS spectra of fresh Ag/Al_2O_3 (a) and Ag/TiO_2–Al_2O_3 (b) at various temperatures. Gas composition: 1000 ppm NO, 1000 ppm C_3H_6, 8% O_2, N_2 as balance gas.

The results in Fig. 10 show that the mainly intermediate species are nitrite (NO_2^-), nitrate (NO_3^-), partially oxidation hydrocarbon ($HCOO^-$ and $RCOO^-$) and CN, NCO species. Based on previous study [9,17], the bands in figure are assigned to bands of nitrite (NO_2^-, 1235 cm^{-1}), Monodentate nitrate (1250, 1550 cm^{-1}), bidentate nitrate (1300, 1590 cm^{-1}), and bridge nitrate (1613 cm^{-1}), Acetate species (1460, 1580 cm^{-1}), Formate species (3005, 2905, 1377cm^{-1}) and CN (2154 cm^{-1}), NCO species (~2235 cm^{-1}). On the one hand, there are some common features in DRIFTS spectra of Ag/Al_2O_3 and Ag/TiO_2–Al_2O_3. The appearance of adsorbed NO_2^- and NO_3^- species were observed even at the low temperature of 373 K, and disappeared at the high temperature above 673 K. Formate (3005, 2905, 1380cm^{-1}) and CN species reached the maximum value around 573 K, and the intensity decreased above and below this temperature. Acetate species (1460, 1580 cm^{-1}) were not detected at low temperature, but appeared at 573 K, and the intensity increased as the temperature increase.

On the other hand, some differences were discerned in DRIFTS spectra of Ag/Al_2O_3 and Ag/TiO_2–Al_2O_3. First, the intensity of NO_2^- species (1235 cm^{-1}) and Monodentate nitrate (1250 cm^{-1}) on Ag/Al_2O_3 was much higher than that on Ag/TiO_2–Al_2O_3 at low temperature, and these species, which should be defined by weak NO_x adsorption, was almost not detected at 373 K on Ag/TiO_2–Al_2O_3. The intensities of nitrate species (1618, 1570, 1592, 1300 cm^{-1}) were high on Ag/TiO_2–Al_2O_3 at low temperatures (below 473 K) compared to Ag/Al_2O_3. These results are in accordance with the result of TPD of NO (see Fig. 6), the amount of weak NO_x adsorption species were small on Ag/TiO_2–Al_2O_3 compared to Ag/Al_2O_3, and the peak at high temperature on Ag/TiO_2–Al_2O_3 shifted about 100 K to lower temperature compared to that of Ag/Al_2O_3. As shown in Fig. 11, in addition, the intensities of formate (3005, 2905 cm^{-1}) at 573 K over Ag/TiO_2–Al_2O_3 were higher than on Ag/Al_2O_3. This may be the reason for the difference of NO conversion. Furthermore, CN (2154 cm^{-1}) as one of key intermediates of HC-SCR was also much stronger over Ag/TiO_2–Al_2O_3 than on Ag/Al_2O_3, although significant NCO specie was not observed at 573 K over Ag/TiO_2–Al_2O_3.

The in situ DRIFTS spectra of the aged catalysts in the flow of $NO + C_3H_6 + SO_2 + O_2$ at steady-state at various temperatures were studied in detail. For the purpose of easy comparison, only the results over fresh and aged catalyst at 523 and 723 K were shown in Fig. 12. According to the literature [33], the band at 1360 cm^{-1} could be attributed to asymmetric stretching vibrations of O═S═O, while the band at 1160 cm^{-1} could be attributed to the symmetric stretching vibrations of O═S═O. In the dynamic test, the intensity of sulfate species increased steadily as SO_2 was injected into the feed. Nitrate species (1250, 1588, 1300 cm^{-1}) were covered by other species, that is, nitrate species could hardly form on the aged catalyst. However, at the low temperature of 523 K, the peaks of the formate species (3002, 2905 cm^{-1}) were enhanced on the aged sample, and acetate species (1590, 1467 cm^{-1}) also increased. Furthermore, the key intermediate species, –NCO (2230, 2260 cm^{-1}) and –CN (2160 cm^{-1}) were also promoted on the aged catalyst at low temperature. The intensities of these species, however, did not change at the high temperature of 723 K.

4. Discussion

4.1. Activity enhancement on Ag/TiO_2–Al_2O_3

Ag-based catalysts on various supports of single metal oxide TiO_2, Al_2O_3 and binary metal oxide TiO_2–Al_2O_3 showed obvious differences in selective catalytic reduction of NO with propene. With TiO_2 support, the catalytic activity is very low (<10%). This is probably due to the lowest specific area of TiO_2 among these catalysts (see Table 1.). Furthermore, it is so difficult to adsorb the reaction gas on the surface of the catalyst that the amount of NO_x adsorption in TPD is less than 15% of the amount on Ag/TiO_2–Al_2O_3. The in situ DRIFTS spectra of Ag/TiO_2 are almost linear (Fig. 11). This result suggests that little intermediates are adsorbed and formed on the surface of Ag/TiO_2, leading to the lowest activity among these catalysts. Silver supported on γ-Al_2O_3 showed good activity for SCR of

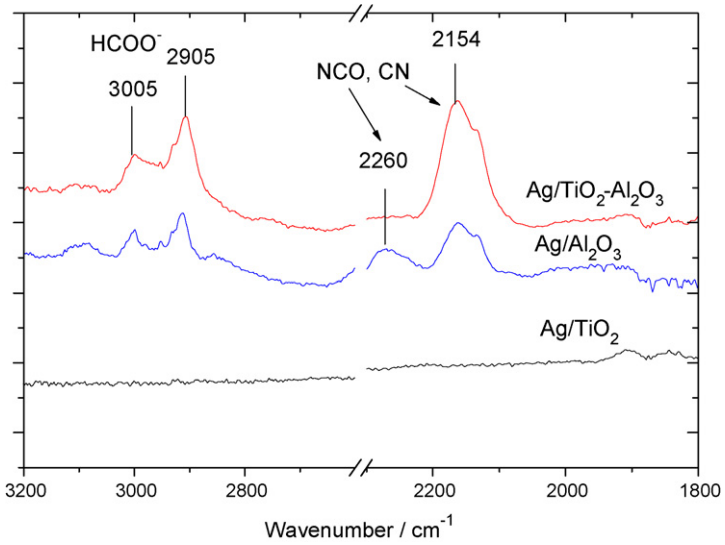

Fig. 11. Comparison of some key species in in-situ DRIFTS spectra on various fresh catalysts, Ag/Al_2O_3, Ag/TiO_2 and Ag/TiO_2–Al_2O_3. Reaction temperature: 573 K; gas composition: 1000 ppm NO, 1000 ppm C_3H_6, 8% O_2, N_2 as balance gas.

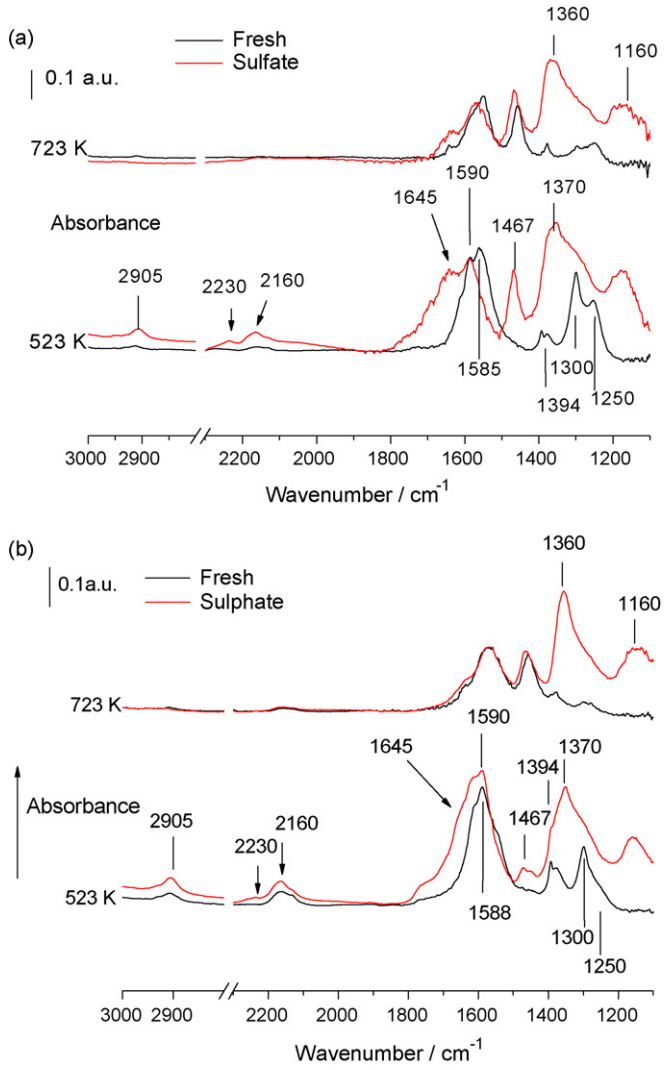

Fig. 12. In-situ steady-state DRIFTS spectra of fresh and aged catalysts. (a) Ag/Al_2O_3, (b) Ag/TiO_2–Al_2O_3. Gas composition: 1000 ppm NO, 1000 ppm C_3H_6, 8% O_2, 0 or 100 ppm SO_2, N_2 balance.

NO with propene (Fig. 1), similar to the results reported by many other researchers [9–13].

It is important that the catalytic activities were greatly enhanced by using the binary metal oxide TiO_2–Al_2O_3 composite as the support, especially at the low temperature region (see Fig. 1). BET results showed that the surface of Ag/TiO_2–Al_2O_3 did not decrease and its average pore diameter and pore volume greatly increased compared to Ag/Al_2O_3. The XRD and TEM results indicated that the combination of anatase TiO_2 and γ-Al_2O_3 formed an amorphous system due to no separate anatase titania and gamma alumina crystal structure observed, although the composite solid solution was not obtained due to the same value of the Ti2p and Al2p binding energy detected in XPS (Table 2). In addition, XPS results showed that the concentration of surface oxygen of Ag/TiO_2–Al_2O_3 increased, which probably promotes the activation of propene and adsorption of NO_x. More importantly, the active component of silver was well dispersed in the TiO_2–Al_2O_3 amorphous system compared to that on Al_2O_3 (Fig. 4); the intensity of Lewis acid sites on the TiO_2–Al_2O_3 amorphous system was higher than on Ag/Al_2O_3. Actually, these different physical properties are the essential reasons for the higher activity on Ag/TiO_2–Al_2O_3 than that on Ag/Al_2O_3 (Fig. 1).

The well-dispersed silver on TiO_2–Al_2O_3 is the likely reason for the highest NO conversion at the low temperatures. This is due to the enhancement of activation of propene to the partial oxidation of intermediate species, such as formate ($HCOO^-$) (Fig. 11). The increase of Lewis acid sites might also be an important contributor to the enhancement of activity over the composite TiO_2–Al_2O_3 amorphous system, especially in the low temperature region. Regarding the ad-NO_x species, the weak adsorption species which includes nitrite (NO_2^-) was the main NO_x adsorption species on the Ag/Al_2O_3 support at low temperatures; however, little of this specie was observed on Ag/TiO_2–l_2O_3. In contrast, the strong adsorption species of NO_3^- on Ag/TiO_2–Al_2O_3 were much higher than on Ag/Al_2O_3 (Fig. 6). Considering the catalytic activities, although little NO_x

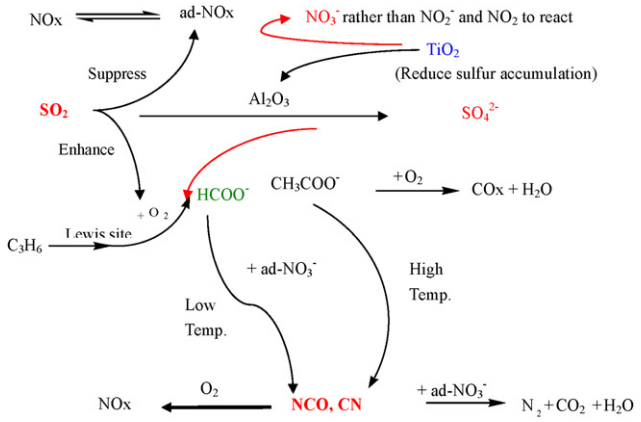

Fig. 13. Proposed reaction pathway and enhanced mechanism of SCR over Ag/TiO_2–Al_2O_3.

is adsorbed over Ag/TiO_2–Al_2O_3, its activity is much higher than that of Ag/Al_2O_3 below 673 K. Therefore, the crucial ad-NO_x species for SCR of NO with propene is probably a strong NO_x adsorption species such as NO_3^- instead of NO_2^-, and the ad-NO_3^- species desorbed above 523 K are presumed to participate in NO reduction reactions (Fig. 13).

Furthermore, CN (2154 cm^{-1}) as one of key intermediates of HC-SCR is much stronger over Ag/TiO_2–Al_2O_3 than that over Ag/Al_2O_3. NCO, however, one of important species in the HC-SCR on Ag/Al_2O_3, was not observed over Ag/TiO_2–Al_2O_3, which is probably due to the instability of NCO in that it easily reacts with ad-NO_x to form N_2. With the temperature above 773 K, the catalytic activity decreased even where the acetate species was abundant (1467 cm^{-1}) and the feed gas contained NO but little nitrate species formed. As shown in the Fig. 13, NO_3^- instead of NO_2^- and NO in HC-SCR, is essential to react with oxygenate intermediates such as formate and acetate to generate CN or NCO which then quickly reacts with ad-NO_3^- to form N_2.

4.2. Effect of SO_2 on catalyst performance

SO_2 inevitably exists in the exhaust gas from vehicle and poisons the catalyst, the application of lean NO_x catalysts including lean NO_x trap and HC-SCR has been hindered.

On a fresh catalyst, the maximum activities were slightly suppressed in the presence of SO_2. Because the accumulation of surface sulfate species is a steady process in the presence of SO_2, there is little sulfate formation on the fresh catalyst. The activity decrease was mainly due to the competitive adsorption of SO_2 with the NO on the surface of catalyst. TPD of NO showed that when NO adsorption occurred together with SO_2, the amount of nitrate species decreased from 235 to 126 μ mol g^{-1} on Ag/Al_2O_3. If the concentration of SO_2 were low, such as 50 ppm, the competitive adsorption was too weak to affect the reaction [13,21].

On an aged sample, the maximum NO conversion decreased significantly in the presence of SO_2. The reason is mainly due to the sulfate species that formed on the surface of catalysts blocking the adsorption of NO. The surface sulfate species undergo little decomposition and inhibit the active sites. This suggests that the surface sulfate species were more stable than nitrates and occupied the alkali adsorption sites on these catalysts to baffle the adsorption of NO. The sulfate species were also detected in EDS tests and FT-IR, and the formation of sulfate on the surface of catalyst led to the decrease of surface area. In the TPD of NO, the results indicated that the formation of sulfate arrested the adsorption of NO_3^- in the high temperature region, although it seemed that the formation of the surface sulfate species could help to form NO_2^- on Ag/Al_2O_3 at low temperature.

In DRIFTS results, the intensity of sulfate species on aged catalysts was much more than that of other species, and these sulfate species could adsorb across wide temperature range from 473 to 873 K. This result can also be supported by the TPD results of SO_2 (Fig. 7). It can be suggested that, the combination of the surface sulfate species and the type of support was much stronger than that of the nitrate species. It is, therefore, likely that the formation of surface $Al_2(SO_4)_3$ inhibited the NO activity of the SCR because the formation of surface Ag_2SO_4 did not affect the activity but played a promotional role [13].

However, the catalytic activity was greatly enhanced in the low temperature range. Based on Py-IR studies, the formation of the sulfate species enhanced the acid site which was important for the activation of C_3H_6 to carboxylate species, such as formate and acetate. The formate and CN, NCO species were obviously enhanced on the aged catalyst at 523 K (Fig. 12). The results supported the suggestion that the key species, CN and NCO, were indeed involved in the catalytic reduction of NO [9,34–36].

Based on the previous reports, it seems that there are two ways to improve the sulfur-resistance for lean NO_x reduction. One is to integrate the catalytic material with high activity onto an aged catalyst, such Ag_2SO_4 [13]. The other is to develop a sulfur resistant alumina material. TiO_2–Al_2O_3 composite amorphous support seems to be reasonably sulfur resistant as it shows little sulfate formation and high NO selective adsorption compared to alumina. The elemental concentration of S on aged Ag/TiO_2–Al_2O_3 was less than half that of the Ag/Al_2O_3 catalyst, and the amount of decreased specific area was also lower than that of Ag/Al_2O_3. Furthermore, the amount of NO_x adsorption at the high temperature range of 373–873 K on aged Ag/TiO_2–Al_2O_3 was still much higher than that on Ag/Al_2O_3, whereas TPD of SO_2 showed that less SO_2 adsorption occurred on composite amorphous TiO_2–Al_2O_3 which also formed less sulfate alumina. These results indicated that composite amorphous TiO_2–Al_2O_3 probably suppressed the formation of surface sulfur species and then reduced the negative effects of SO_2.

The above discussions are summarized in the schematic reaction scheme shown in Fig. 13. NO is formed as nitrate on the surface of catalyst, while propene is partially oxidized on the Lewis acid sites to formate or acetate or other oxygenated species. NO_3^- rather than NO_2^- or NO_x will react with the carboxylate species to generate CN or NCO, which then quickly react with ad-NO_3^- to produce N_2 and CO_2. Formate specie is easy to react with nitrate to form CN and NCO at low

temperatures, while acetate specie is abundantly existed at high temperature. Incorporating TiO_2 to Al_2O_3 increased the number of Lewis acid sites, on which the amount of formate ($HCOO^-$) and CN increased, and then the activity was enhanced at low temperatures. Sulfate species enhanced the intensity of Lewis acid site while suppressed the adsorption of NOx on the surface of the catalyst. Therefore, the catalytic activities were enhanced at low temperatures while the maximum NO conversion significantly decreased on aged samples due to the accumulated sulfate species on the surface of catalysts. The addition of TiO_2 on Al_2O_3 promoted the formation of NO_3^-, however, the rate of sulfate accumulation in the Ag/TiO_2–Al_2O_3 amorphous system decreased, and showed much more capability for selective adsorption of NO and toleration to SO_2 than that of Ag/Al_2O_3.

5. Conclusions

The supports, Al_2O_3, TiO_2 and binary metal oxide TiO_2–Al_2O_3 exerted an influence on catalytic activities in HC-SCR. Catalytic activity was greatly enhanced for the Ag/TiO_2–Al_2O_3 support in the low temperature region. Ag/TiO_2–Al_2O_3 prepared by the sol–gel method is an amorphous composite, and the active component of silver was well dispersed in the amorphous system. The large specific area, pore volume and pore diameter caused high NO adsorption (NO_3^-). The enhancement of Lewis acid sites seems to provide the highest NO conversion due to the promotion of activation of propene to partial oxidation intermediate species, such as formate ($HCOO^-$). CN, as one of key intermediates of HC-SCR, is much stronger over Ag/TiO_2–Al_2O_3 than over Ag/Al_2O_3. NO_3^- instead of NO_2^- and NO in HC-SCR is essential since it reacts with oxygenate intermediates.

The effects of SO_2 were mainly due to the formation of surface sulfate species and the competitive adsorption between SO_2 and NO. The activity decrease on a fresh catalyst in the presence of SO_2 was mainly due to the competitive adsorption of SO_2 with the NO. The maximum NO conversion was reduced significantly on an aged sample due to the sulfate species (i.e. $Al_2(SO_4)_3$) formed on the surface of catalysts. This surface sulfate undergoes little decomposition, thus inhibiting the active sites. On the other hand, the catalytic activities were greatly enhanced at the low temperature range. The formation of sulfate species obviously enhanced the intensity of Lewis acid site, which was important for the activation of C_3H_6 to carboxylate species. The Ag/TiO_2–Al_2O_3 composite amorphous seemed to reduce the rate of sulfate formation to some extent, and showed the higher capability of NO selective adsorption compared to alumina. These behaviors led to a high tolerance to SO_2 on Ag/TiO_2–Al_2O_3 and then reduce the negative effects of SO_2.

Acknowledgements

This work was financially supported by National Natural Science fund of China (grant nos. 20507012 and 20437010) and National High Science & Technology Project (863, grant no. 2006AA060301).

References

[1] M. Iwamoto, H. Hamada, Catal. Today 10 (1991) 57.
[2] H. Akama, K. Matsushita, Catal. Surv. Jpn. 3 (1999) 139.
[3] R. Burch, J.P. Breen, F.C. Meunier, Appl. Catal. B 39 (2002) 283.
[4] G.B.F. Seijger, P.V.K. Niekerk, K. Krishna, H.P.A. Calis, H.V. Bekkum, C.M.V. Bleek, Appl. Catal. B 40 (2003) 31.
[5] C. Shi, M. Cheng, Z. Qu, X. Yang, X. Bao, Appl. Catal. B 35 (2002) 173.
[6] A.A. Nikolopoulos, E.S. Stergioula, E.A. Efthimiadis, I.A. Vasalos, Catal. Today 54 (1999) 439.
[7] P. Carniti, A. Gervasini, V.H. Modica, N. Ravasio, Appl. Catal. B 28 (2000) 175.
[8] G. Ferraris, G. Fierro, M.L. Jacono, M. Inversi, R. Gragone, Appl. Catal. B 45 (2003) 91.
[9] F.C. Meunier, J.P. Breen, V. Zuzaniuk, M. Olsson, J.R.H. Ross, J. Catal. 187 (1999) 493.
[10] F.C. Meunier, J.R.H. Ross, Appl. Catal. B 24 (2000) 23.
[11] S. Satokawa, K. Yamaseki, H. Uchida, Appl. Catal. B 34 (2001) 299.
[12] F.C. Meunier, V. Zuzaniuk, J.P. Breen, M. Olsson, J.R.H. Ross, Catal. Today 59 (2000) 287.
[13] P.W. Park, C.L. Boyer, Appl. Catal. B 59 (2005) 27.
[14] K. Masuda, K. Tsujimura, K. Shinoda, T. Kato, Appl. Catal. 8 (1996) 33.
[15] T. Zhu, J. Hao, W. Li, Chem. Lett. (2000) 478.
[16] H. He, Y. Yu, Catal. Today 100 (2005) 37.
[17] H. He, J. Wang, Q. Feng, Y. Yu, K. Yoshida, Appl. Catal. B 46 (2003) 365.
[18] I.H. Son, M.C. Kim, H.L. Koh, K.-L. Kim, Catal. Lett. 75 (2001) 191.
[19] S. Sumiya, M. Saito, H. He, Q.-C. Feng, N. Takezawa, Catal. Lett. 50 (1998) 87.
[20] H.S. Gandhi, M. Shelef, Appl. Catal. 77 (1991) 175.
[21] T.N. Angelidis, S. Christoforou, A. Bongiovanni, N. Kruse, Appl. Catal. B 39 (2002) 197.
[22] G.M. Dhar, B.N. Srinivas, M.S. Rana, M. Kumar, S.K. Maity, Catal. Today 86 (2003) 45.
[23] J. Ramirez Diaz, G. Fuentes, M. Vrinat, M. Breysse, M. Lacroix, Appl. Catal. 52 (1989) 211.
[24] J. Ramirez, A. Gutierrez, Alejandre, J. Catal. 170 (1997) 108.
[25] J.H. Li, J.M. Hao, L.X. Fu, Z.M. Liu, X.Y. Cui, Catal. Today 90 (2004) 215.
[26] J.H. Li, H.J. Fu, L.X. Fu, J.M. Hao, Environ. Sci. Technol. 40 (2006) 6455.
[27] J.H. Li, J.M. Hao, L.X. Fu, Z.M. Liu, X.Y. Cui, Appl. Catal. A 265 (2004) 43.
[28] J.H. Li, J.M. Hao, L.X. Fu, X.Y. Cui, Catal. Lett. 103 (2005) 75.
[29] J.A. Dean, Lange's Handbook of Chemistry (15th), McGraw-Hill Book Co., 2003.
[30] M. Haneda, Y. Kintaichi, H. Hamada, Appl. Catal. B 31 (2001) 251.
[31] C. Morterra, G. Cerrato, V. Bolis, Catal. Today 17 (1993) 505.
[32] K. Fottinger, K. Zorn, H. Vinek, Appl. Catal. A 284 (2005) 69.
[33] J.M. Watson, U.S. Ozkan, J. Catal. 217 (2003) 1.
[34] M. Haneda, E. Joubert, J. Menezo, D. Duprez, J. Barbier, N. Bion, M. Daturi, J. Saussey, J.C. Lavalley, H. Hamada, J. Mol. Catal. A 175 (2001) 179.
[35] T.M. Orlando, A. Alexandrov, A. Lebsack, J. Herring, J.W. Hoard, Catal. Today 89 (2004) 151.
[36] H. He, C. Zhang, Y. Yu, Catal. Today 90 (2004) 191.